Defence Science Journal, Vol. 71, No. 6, November 2021, pp. 836-845, DOI : 10.14429/dsj.71.17219

Modelling and Analysis of Laser Beam-rider Guided Tank Ammunition with a Diameter of 155 mm

Mehmet Kum[@], Haluk Gözde[#], and Semih Özden[#,*]

[@]*National Defence University, Alparslan Defence Sciences Institute, Electronic Warfare Program, Ankara, Turkey*
[#]*National Defence University, Turkish Military Academy, Department of Electronics and Communication Engineering, Ankara, Turkey*
[*]*E-mail: sozden@kho.edu.tr*

ABSTRACT

On the battlefield of today, it has become an important requirement to hit moving or fixed targets by using tank or artillery ammunition with high precision. However, while there are many articles on guiding tactical missiles, it cannot found sufficient scientific study for guiding tank ammunition in the related literature. In this study, the laser BR-guidance method is offered to the classic tank ammunition with a diameter of 155 mm in order to give the tank a precision strike capacity, as different from the literature. First of all, an ammunition model is created with coefficients of the mass, inertia, and surface area and friction. In addition, an autopilot dynamic is modelled for the pitch and roll axes of the ammunition. Also, the atmosphere model and environmental factors are added to the model. In order to control this nonlinear model, a lead-compensator and a PD-controller are designed. In order for the results to be transferred to a real application, the accelerations obtained must basically be produced by the electric motors that will drive the control surfaces to be designed. At the end of the study, it is seen that both controllers can produce lateral accelerations within limits without reaching high saturation.

Keywords: Tank ammunition; Beam-rider guidance; Dynamic modelling; Lead compensator; PD-controller

1. INTRODUCTION

Traditional tank and artillery ammunition used in front-line warfare aims to hit the target using basic projectile shooting principles. In conventional warfare, this ammunition is often used to suppress an area and does not require high accuracy of shooting. However, due to the changing war environment and threats, it has become an important necessity to hit moving or fixed targets with tank or artillery ammunition with high precision in today's battlefield. Especially in a tank battle, it is vital to hit a moving enemy tank with high accuracy on the first shot. The precision shooting feature of tank or artillery ammunition can be achieved by applying guidance methods thanks to today's advanced electromechanical and microelectronic technology. In this way, artillery or tank ammunition, which provides guided weapons capability, can neutralise enemy targets both by using less ammunition and in the first shot that ensures survival.

There are several well-known guidance methods in the literature[1]. Among these, two guidance methods come to the fore in the guidance of tank or artillery ammunition. The first is laser-guided ammunition that hit the point indicated by a laser pointer and operates according to the geometry of the semi-active homing. The other is the Beam-Rider (BR) geometry where the ammunition reaches the target by riding the laser beam. The BR-guidance method was started to be applied in the early stages of the guided missile systems because it was developed both as hardware and software simpler and more convenient than other guidance methods[2-3]. When the related literature is examined, it is seen that there are few studies about BR-guidance and they are generally used for tactical missiles[4]. For example, Maryniak[5], *et al.* offered the dynamic performance of BR-guidance method used in a missile system by using Maggi equations[6] in 2005. Wang[7], *et al*. developed an integrated guidance control system for BR guided missile in 2009. After that, Mingliang[8], *et al*. applied the BR-guidance method to the artillery missile system in 2014. After one year, Zhou[9], *et al*. studied 980nm diode laser for improving the performance of laser BR guided system. In 2018, Wang[10], *et al*. suggested the generation method for information based optical phased array of a laser BR guidance system. It is clear that it is difficult to find open source publications on this subject, and there is no design study to apply laser BR-guidance to the tank ammunition.

As different from the literature, the BR-guidance method is applied to the tank ammunition in order to provide precision shooting capability to the mobile tank. In this way, it is aimed to hit the moving enemy tank with high accuracy at the first shot in a tank war. For this purpose, the issue of gaining guidance capability by applying the laser BR-guidance method to general purpose tank ammunition with a diameter of 155 mm is

Received : 16 June 2021, Revised : 06 August 2021
Accepted : 25 August 2021, Online published : 22 October 2021

examined. First of all, an ammunition model is created by using the mass, inertia, and surface area and friction coefficients of this ammunition in open source. By combining these values and the speed and maneuver information of possible targets, guidance simulation is performed in MATLAB/Simulink environment with the assumption of 3D point mass modelling. The simulation is solved with the 4th order Runge-Kutta method by creating a target function for guidance control. In addition, autopilot dynamics for the pitch and roll axes of the tank ammunition is modelled, and the atmosphere model and environmental factors are also added to the model to make the simulation environment more realistic. For the BR-guidance control, a lead-compensator and a Proportional Derivative (PD) controller are designed. The performance of the guidance control method is verified with three different scenarios including moving and fixed targets.

The article is organised as follows: first, complete modelling of BR-guidance system is given in detail. Second, the results and the comprehensive discussion are presented. Finally, the conclusion contains recommendations for further studies.

2. BEAM-RIDING GUIDANCE MODELLING

Guidance is the process of guiding a moving object according to the desired path or destination. There are various guidance methods in the literature with different advantages and disadvantages[1-3]. One of them is Command Line-of-Sight (CLOS) guidance, which is a relatively cost-effective method developed for high-performance hits. Basically, the missile aims to stay on the LOS marked towards the target[11]. CLOS guidance method is also known as the three-point guidance rule because it consists of three components: marker, missile and target. Marking can be done with narrow beam radar or coded laser signal. On the back of the missile, there are sensors to detect the signal being marked[11]. Guidance commands are calculated on the marker platform and transmitted to the missile via cable or a wireless data link. The biggest advantage of this method is its high hit rate, as it is followed by sight. The disadvantages are that the marked signal cannot follow the target by scattering over long distances and it cannot follow the target in escape maneuvers. That is, the CLOS guidance method works more effectively against short-range, fixed-speed targets.

BR-guidance is a semi-automatic CLOS guidance method. Generally, the laser receiver receives the signal sent from the marker and generates angle difference with respect to the LOS axis. Also, a GPS/INS unit measures the position of the missile relative to the reference axis. Then, the guidance processing unit generates lateral acceleration commands. Finally, the autopilot unit converts the acceleration commands from the guidance unit into angle commands and sends to the control surfaces[11-12]. In this study, the BR-guidance method is applied to the classic tank ammunition to provide precise targeting capability.

2.1 Ammunition Model

The ammunition guided BR method tries to stay on the laser beam emanating from the marker. For this purpose, the guidance rule generates lateral acceleration commands that will minimise the distance relative to this beam. Thus, the lateral acceleration commands in 3D Cartesian coordinates as presented in Fig. 1 are calculated as follows;

In the one-axis block diagram, R_M is the distance to the estimated marker measured via the GPS/INS systems on the ammunition. Also, θ_m and θ_T are the ammunition and target angles from the reference, d is missing distance and K is guidance constant. When the lateral acceleration is produced, K is directly proportional to the ammunition distance, while the oscillation frequency of the lateral acceleration is inversely proportional. Therefore, K controller alone is not sufficient to reduce the missing distance. For this reason, better results should be obtained by adding a $G(s)$ controller transfer function to the system. The position of the ammunition in the Cartesian coordinates and the angles with respect to these axes are formulated as follows;

$$\dot{x}_M = V_M \cos\gamma_M \cos\phi_M \quad (1)$$

$$\dot{y}_M = V_M \cos\gamma_M \sin\phi_M \quad (2)$$

$$\dot{z}_M = V_M \sin\gamma_M \quad (3)$$

$$\dot{R}_{OM} = V_M \cos\gamma_M \cos\gamma_{OM} \cos\left(\phi_M - \phi_{OM}\right) + V_M \sin\gamma_M \sin\gamma_{OM} \quad (4)$$

$$\dot{\phi}_{OM} = \frac{V_M \cos\gamma_M \sin\left(\phi_M - \phi_{OM}\right)}{R_{OM} \cos\gamma_{OM}} \quad (5)$$

$$\dot{\gamma}_{OM} = \frac{-V_M \cos\gamma_M \sin\gamma_{OM} \cos\left(\phi_M - \phi_{OM}\right)}{R_{OM}} + \frac{V_M \sin\gamma_M \cos\gamma_{OM}}{R_{OM}} \quad (6)$$

$$\dot{\phi}_M = \frac{a_{y_M}}{V_M \cos\gamma_M} \quad (7)$$

$$\dot{\gamma}_M = \frac{a_{p_M}}{V_M} \quad (8)$$

where R_{OM}, ϕ_M, γ_M, ϕ_{OM}, γ_{OM} denote the range, yaw and pitch angles, yaw and pitch axis LOS angles of the ammunition, respectively. Likewise, R_{OT}, ϕ_T, γ_T, ϕ_{OT}, γ_{OT} denotes the range, yaw and pitch angles, yaw and pitch axis LOS angles of the target. Accordingly, the lateral accelerations of the yaw and pitch axes for the ammunition are calculated as follows[13];

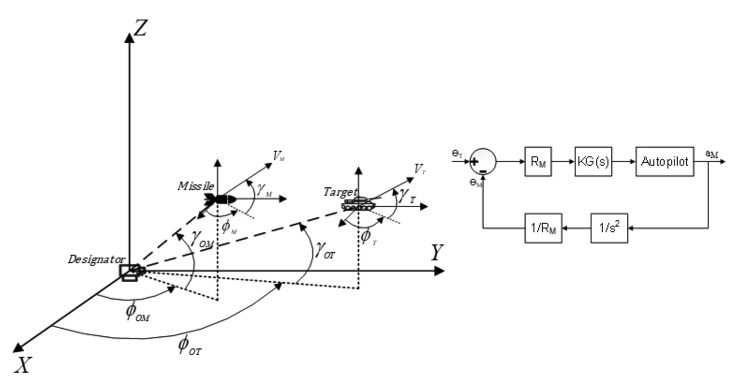

Figure 1. 3D geometry (left) and one-axis block diagram (right) of BR-guidance.

$$a_{y_M} = K_y G(s) R_M \cos\gamma_{OM} \left(\phi_{OT} - \phi_{OM}\right) \tag{9}$$

$$a_{p_M} = K_p G(s) R_M \left(\gamma_{OT} - \gamma_{OM}\right) \tag{10}$$

2.2 Target Model

The position of the target in the Cartesian coordinates and the angles with respect to these axes are calculated as follows;

$$\dot{x}_T = V_T \cos\gamma_T \cos\phi_T \tag{11}$$

$$\dot{y}_T = V_T \cos\gamma_T \sin\phi_T \tag{12}$$

$$\dot{z}_T = V_T \sin\gamma_T \tag{13}$$

$$\dot{R}_{OT} = V_T \cos\gamma_T \cos\gamma_{OT} \cos\left(\phi_T - \phi_{OT}\right) + V_T \sin\gamma_T \sin\gamma_{OT} \tag{14}$$

$$\dot{\phi}_{OT} = \frac{V_T \cos\gamma_T \sin\left(\phi_T - \phi_{OT}\right)}{R_{OT} \cos\gamma_{OT}} \tag{15}$$

$$\dot{\gamma}_{OT} = \frac{-V_T \cos\gamma_T \sin\gamma_{OT} \cos\left(\phi_T - \phi_{OT}\right)}{R_{OT}} + \frac{V_T \sin\gamma_T \cos\gamma_{OT}}{R_{OT}} \tag{16}$$

$$\dot{\phi}_T = \frac{a_{y_T}}{V_T \cos\gamma_T} \tag{17}$$

$$\dot{\gamma}_T = \frac{a_{p_T}}{V_T} \tag{18}$$

a_{y_T} and a_{p_T} are the lateral accelerations of the yaw and pitch axes generated for the target, respectively.

2.3 Acceptances for the Modelling

- The initial conditions of ϕ_M is taken as the angle that the tank barrel makes with the Y axis, γ_M is taken as the elevation angle of the tank barrel, ϕ_{OM} and γ_{OM} are found by calculation depending on the initial position of the ammunition.
- The x_M, y_M and z_M positions are taken as the barrel position based on the Leopard-2 tank dimensions presented in Fig. 2[14].
- The a_{y_M} and a_{p_M} acceleration commands are limited to 50g, which is the limit the ammunition can perform and withstand.
- V_M is used in different scenarios between 500-700 m/s velocity by looking at the barrel velocity of the tanks in the inventory.
- Considering the possible land targets, the V_T is determined to be accelerated with a maximum of 3 m/s^2 and the maximum speed limit is 160 km/h.
- Among the possible land targets, a 10 m long, 3.5 m wide and 2.5 m high tank is accepted as the largest, and the smallest 5 m long, 2.3 m wide and 2 m high armoured personnel carrier is considered.
- The marking range is determined as a maximum of 5 km.

2.4 Modelling Atmosphere Effects

The COESA atmosphere[15] model in MATLAB software is used. The main purpose of using this model is to obtain the changes in air density and sound velocity depending on altitude. Depending on these changes, the friction force acting on the ammunition is subtracted and the changes in the velocity vector are found. The drag force, the variation of ammunition velocity with the drag force and the disruptive force caused by the wind are calculated as follows[16-17]. In addition, the drag coefficient depending on the velocity of the 155 mm ammunition is given in Table 1[18-19].

$$D_M = 0.5 \rho V_M^2 S C_D \tag{19}$$

$$\dot{V}_M = \frac{-D_M}{m} - g \sin\gamma_M \tag{20}$$

Table 1. Drag coefficient depend on the speed of the ammunition[18-19]

Speed of the ammunition [Mach]	C_D	Speed of the ammunition [Mach]	C_D
0.400	0.138	0.975	0.244
0.600	0.138	1	0.290
0.700	0.139	1.025	0.309
0.750	0.140	1.050	0.329
0.800	0.141	1.1	0.326
0.850	0.148	1.2	0.318
0.875	0.152	1.35	0.305
0.900	0.156	1.500	0.291
0.925	0.177	1.750	0.269
0.950	0.199	2.000	0.249

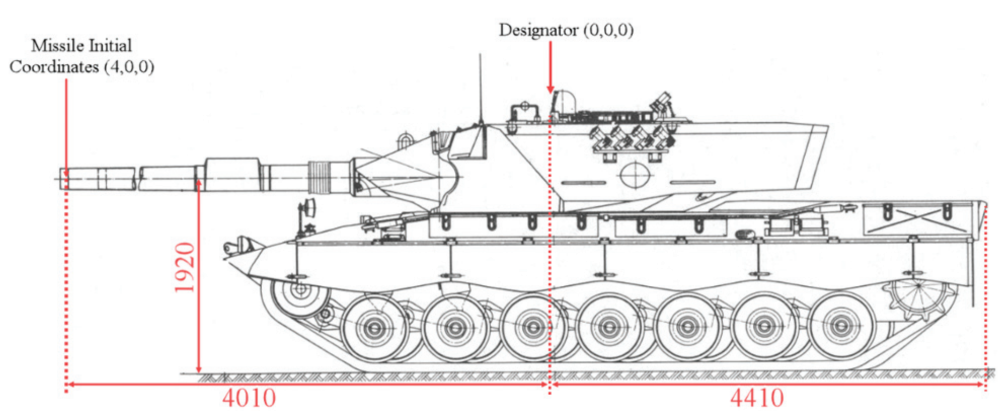

Figure 2. Leopard-2 tank dimensions and the marker position.

$$F_D = 0.5\rho V_R^2 A \tag{21}$$

where m is the mass of the ammunition, g is the gravitational acceleration, ρ is the air density, V_R is the wind speed and A is the ammunition surface area which is calculated in accordance with Baranowski[20].

2.5 Modelling Autopilot Dynamics

The purpose of autopilot modelling is to determine the effects of steady state errors, maximum overshoots and delays on the guidance algorithm due to autopilot dynamics. For this reason, it was accepted as a second order transfer function[3]. Yaw and pitch axes autopilot transfer functions are calculated as follows;

$$G(s)_y = \frac{\omega_{n_y}{}^2}{s^2 + 2\zeta\omega_{n_y} s + \omega_{n_y}{}^2} \tag{22}$$

$$G(s)_p = \frac{\omega_{n_p}{}^2(\tau s + 1)}{s^2 + 2\zeta\omega_{n_p} s + \omega_{n_p}{}^2} \tag{23}$$

ω_{n_y}, ω_{n_p}, ζ and τ are chosen as 23, 3.5, 0.8 and 0.1. Also, the autopilot bandwidth is accepted under damped and 25 Hz.

2.6 Sensor Model

BR guided systems use GPS/INS sensor systems to measure current position. By their nature, these sensors operate at a specific sampling frequency, response time, and accuracy. In this study, by adding white noise and delay to the R_M distance with a mean of 1.1 m and a standard deviation of 0.527, the mentioned uncertainty and delays are included[21]. Also, two sampling time delays are added as a sensor delay.

2.7 Modelling Lead and PD Controllers

The ideal ammunition control loop has oscillations depended on control gain. It also requires an aggressive controller as ammunition moves at high speeds. Therefore, a lead compensator and a PD-controller with low rise time and oscillation reducing effect are selected compared with each other in this study. The other control alternatives are discussed in the conclusion.

After designing the lead compensator, the closed loop transfer functions of the yaw and pitch axes controllers are obtained as follows;

$$\frac{a}{\phi} = \frac{52900s^3 + 52900s^2}{s^5 + 46.8s^4 + 53797s^3 + 58190s^2 + 529s + 5290} \tag{24}$$

$$\frac{a}{\gamma} = \frac{1.225s^3 + 12.25s^2}{s^4 + 5.6s^3 + 12.25s^2 + 1.225s + 12.25} \tag{25}$$

Similarly, after designing the PD-controller, the closed loop transfer functions of the yaw and pitch axes controllers are obtained as follows;

$$\frac{a}{\phi} = \frac{3.997e05s^3 + 3.676e05s^2}{s^5 + 140.4s^4 + 4342s^3 + 5.481s^2 + 3.997e05s + 3.676e05} \tag{26}$$

$$\frac{a}{\gamma} = \frac{8292s^4 + 6439s^3 + 570.7s^2}{s^5 + 73.62s^4 + 393.1s^3 + 9125s^2 + 6439s + 570.7} \tag{27}$$

2.8 Complete Model of the Guidance

The complete model of laser BR-guidance for 155 mm tank ammunition is created in MATLAB/Simulink environment. The model includes ammunition dynamics, target dynamics, autopilot dynamics, LOS connection equations and guidance control blocks as depicted in Fig. 3. These blocks are created by using the equations described above.

To find the yaw and pitch angles of the LOS, it is necessary to calculate the angles that the projection of the LOS axis on the XY plane makes with the X and Y axes, respectively. These differential calculations are performed using Runge-Kutta method. The initial yaw and pitch angles for the ammunition and target are calculated as follows;

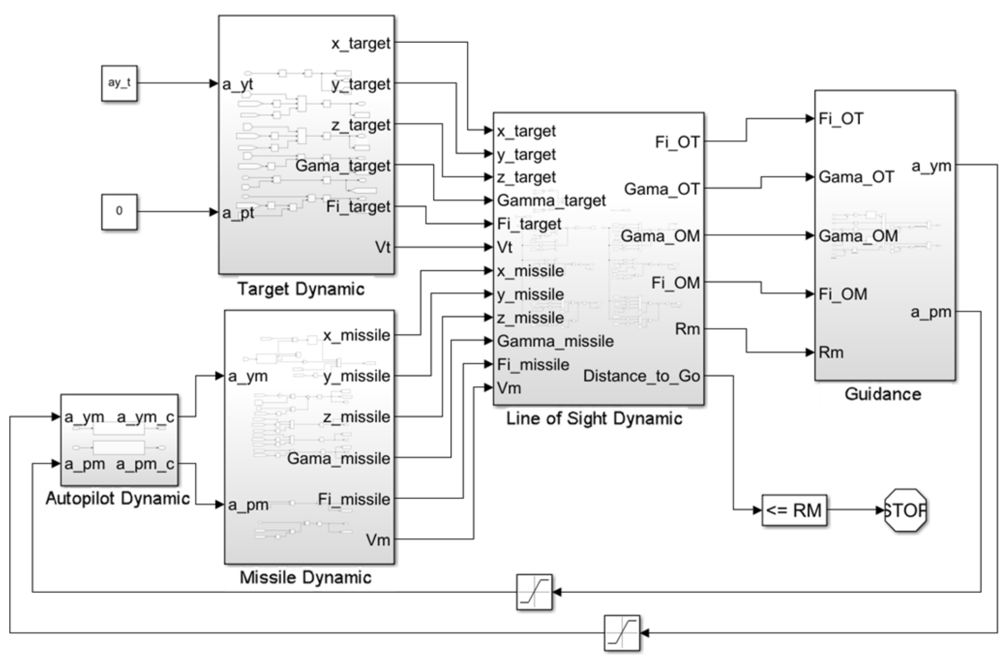

Figure 3. BR-guidance model (above) and its guidance control block (below).

$$\phi_{OM\_0} = \tan^{-1}\frac{y_{M\_0}}{x_{M\_0}} \tag{28}$$

$$\phi_{OT\_0} = \tan^{-1}\frac{y_{T\_0}}{x_{T\_0}} \tag{29}$$

$$\gamma_{OM\_0} = \tan^{-1}\frac{z_{M\_0}}{\sqrt{x_{M\_0}^2 + y_{M\_0}^2}} \tag{30}$$

$$\gamma_{OT\_0} = \tan^{-1}\frac{z_{T\_0}}{\sqrt{x_{T\_0}^2 + y_{T\_0}^2}} \tag{31}$$

As a result of the calculations, the missing distance d to be minimised in the yaw and pitch axes is calculated as follows;

$$d = R_M \cos\gamma_{OM}\left(\phi_{OT} - \phi_{OM}\right) \tag{32}$$

$$d = R_M\left(\gamma_{OT} - \gamma_{OM}\right) \tag{33}$$

3. RESULTS AND DISCUSSION

The war environment has very different scenarios due to its dynamics. In this study, the simulations are made for three different scenarios that could be experienced basically. The ambient conditions and initial values in the scenarios are summarised in Table 2.

The initial pitch and roll angles of the ammunition are considered the same in all scenarios. While creating the scenarios, it is aimed to observe all the factors that could affect the guidance. These factors are the R_M, γ_{OT} and ϕ_{OT}. In order to observe the highest increase and decrease rates of the R_M relative to the starting point, the target is made to move towards and away with 45° angles in the 2th scenarios. Accelerating maneuvers are made in the 3th scenarios to observe the effect of the change in the LOS angles. The obtained results are presented in Figs. 4-6.

In scenario-1, target is considered fixed. Shooting is made at a target 5 km away without lateral wind force. The target is hit with a distance of 0.742 m at the end of 11.46 seconds with the lead controller. The maximum and average accelerations in the pitch and yaw axes are 1.113g and 0.201g, 50.758g and 3.879g, respectively. With the PD controller, the target is hit with a distance of 0.708 m after 11.31 seconds. The maximum and average accelerations in the pitch and yaw axes are 1.101g and 0.220g, 40.689g and 4.044g, respectively.

In scenario-2, the possible land target is approaching with a constant speed of 30 m/s at an angle of 45°. The shoot is carried out under the force of the lateral wind with an angle of 45° on the pitch and roll axes and a speed of 20 m/s to the target at a distance of 5 km. The target is hit with a distance of 1.682 m at the end of 11.07 seconds with the lead controller. The maximum and average accelerations in the pitch and yaw axes were 1.183g and 0.222g, 50,758g and 4.372g, respectively. With the PD controller, the target is hit with a distance of 1.621 m at the end of 11.11 seconds. The maximum and average accelerations in the pitch and yaw axes are 1.104g and 0.244g, 44.084g and 4.554g, respectively.

In scenario-3, the possible land target starts with a speed of 10 m/s and approaches towards the ammunition with a constant acceleration of 3 m/s2 and an angle of 45°. The shoot is carried out under the force of the lateral wind with an angle of 45° on the pitch and roll axes and a speed of 20 m/s to the target at a distance of 5 km. The target is hit with a distance of 2.564m at the end of 9.75 seconds with the lead controller. The maximum and average accelerations in the pitch and yaw axes were 1.265g and 0.267g, 50,759g and 5.441g, respectively. With the PD-controller, the target is hit with a distance of 2.323 m at the end of 9.790 seconds. The maximum and average accelerations in the pitch and yaw axes are 1.196g and 0.295g, 47.656g and 5.560g, respectively.

When the results are examined, it is seen that the ammunition is exposed to high values of lateral yaw acceleration in order to settle on the target LOS axis at the time of first exit in scenario-1. Fortunately, the short-term yaw axis of rotation reaches saturation and achieves target tracking success. Guidance algorithm suppresses the lateral wind force coming to both axes within 2-3 seconds. Since the difference in altitude between the ammunition and the target is small, the pitch axis corrects the climb and provides the orientation to the target. The PD-controller is able to control the errors in the yaw axis with a more stable and low acceleration hysteresis compared to the lead-compensator. In scenario-2, since the target is moving at a constant speed, only the yaw angle changes while the pitch angle remains constant. The tracking performance of the guidance control algorithm decreases and the missing distance increases due to the decrease in the yaw angle. The lead compensator reaches saturation for 0.3 s to minimise the distance caused by the yaw axis of the barrel orientation, and then settles on the LOS. The PD-controller is able to control errors in the yaw axis with a more stable and also lower acceleration hysteresis and lower missing distance compared to the lead compensator. Collision time decreases in proportion to the increase in ammunition speed and the approach of the target. In scenario-3, the target made a parabolic movement with acceleration of 3 m/s^2 and approached towards the ammunition. Accordingly, the LOS axis increases by about 2°. Since the rate of increase is low, guidance algorithms can compensate for this change. Given possible land targets, the results of this scenario have an acceptable success since the missing distances below 2.5 m can be considered successful. Similar to the other scenario results, the PD-controller reaches

Table 2. Scenario conditions

	Target initial point (x, y, z)	Ammunition muzzle velocity (m/s)	Target movement	Wind condition
Scenario 1	3000, 4000, 10	550	Constant	No
Scenario 2	3000, 4000, 10	600	Approach with constant 30 m/s speed and 45° angle	20 m/s (45° 45°)
Scenario 3	3000, 4000, 10	650	Approach with 3 m/s^2 acceleration	20 m/s (45° 45°)

a lower missing distance with less acceleration and oscillation than the lead compensator. The obtained results according to the scenarios are summarised in Table 3.

In general, when examining the performance of the guidance methods, the missing distance, the maximum and average accelerations are taken into account. In order to transfer the results to a real application, the accelerations obtained must be produced by the electric motors that will drive the control surfaces to be designed. Both controllers designed in this context produce lateral accelerations within limits without reaching high saturation. In addition, since the guidance algorithms work according to the angle and distance, the missing distance increases as the target maneuvers and engagement time increase. In the simulations, the Z-axis component dominates the missing distance in all scenarios, as the pitch axis autopilot reduces the aggressiveness of the system.

Finally, the PD controller, together with the derivative effect, reduces the overshoot and oscillations, generating less compelling accelerations to the control surfaces. In addition, it managed to hit the missing distance with less distance than the lead compensator, especially in scenarios where the target moves at constant speed and maneuvers with acceleration. This is due to the estimation property of the derivative in the

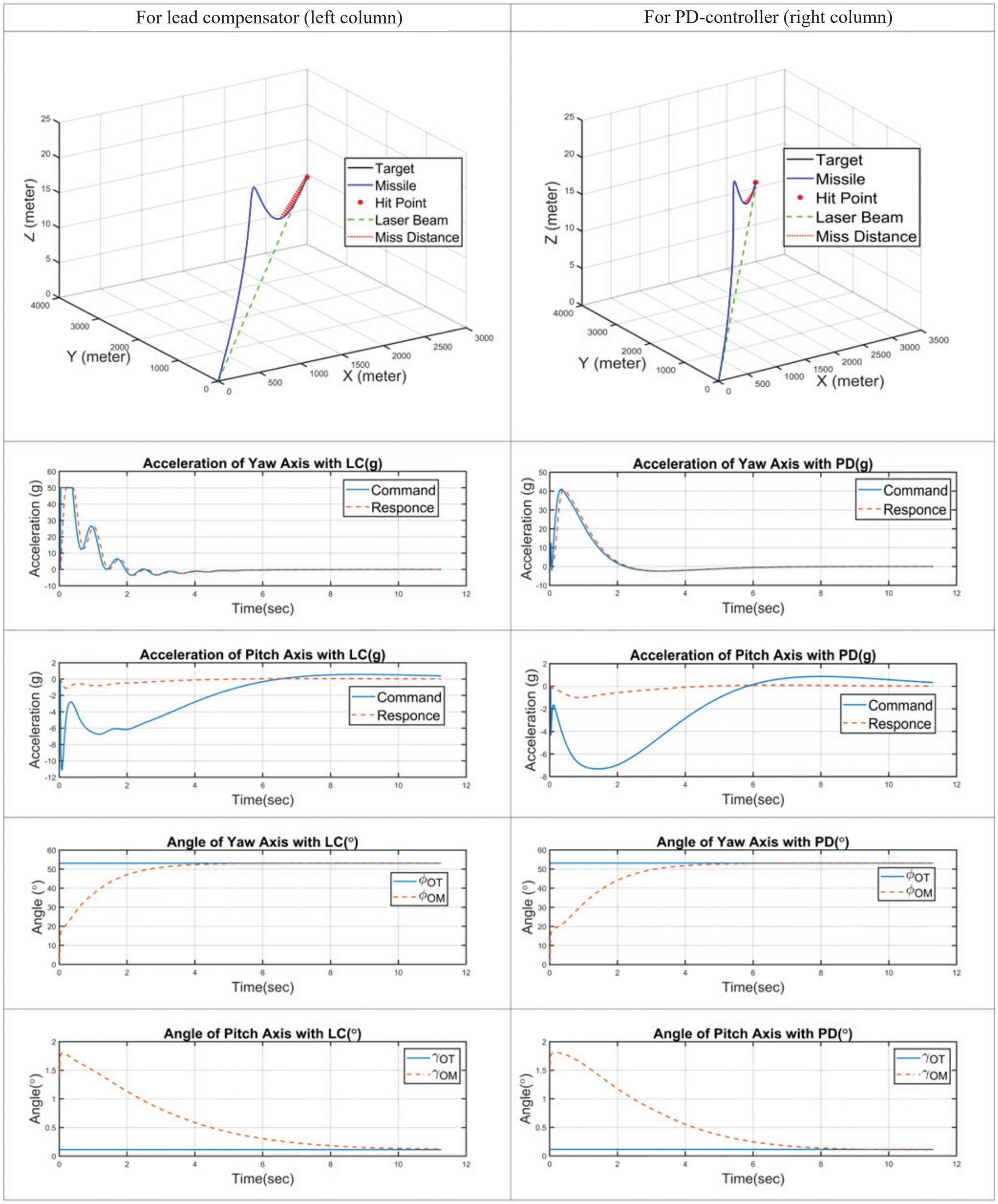

Figure 4. Results for scenario-1 (In order from top to bottom: 3D target and ammunition movements, yaw axis accelerations, pitch axis accelerations, yaw axis LOS angle changes, pitch axis LOS angle changes).

Table 3. Obtained results with respect to the scenarios

	Controller	Miss distance (m)	Average accelerations (g) (Pitch, Yaw)	Maximum accelerations (g) (Pitch, Yaw)
Scenario-1	Lead Compensator	0.742	(0.201, 3.879)	(1.113, 50.758)
	PD-Controller	0.708	(0.220, 40.689)	(1.101, 40.689)
Scenario-2	Lead Compensator	1.682	(0.222, 4.372)	(1.183, 50.758)
	PD-Controller	1.621	(0.244, 4.554)	(1.104, 44.084)
Scenario-3	Lead Compensator	2.564	(0.267, 5.541)	(1.265, 50.759)
	PD-Controller	2.323	(0.295, 5.560)	(1.196, 47.656)

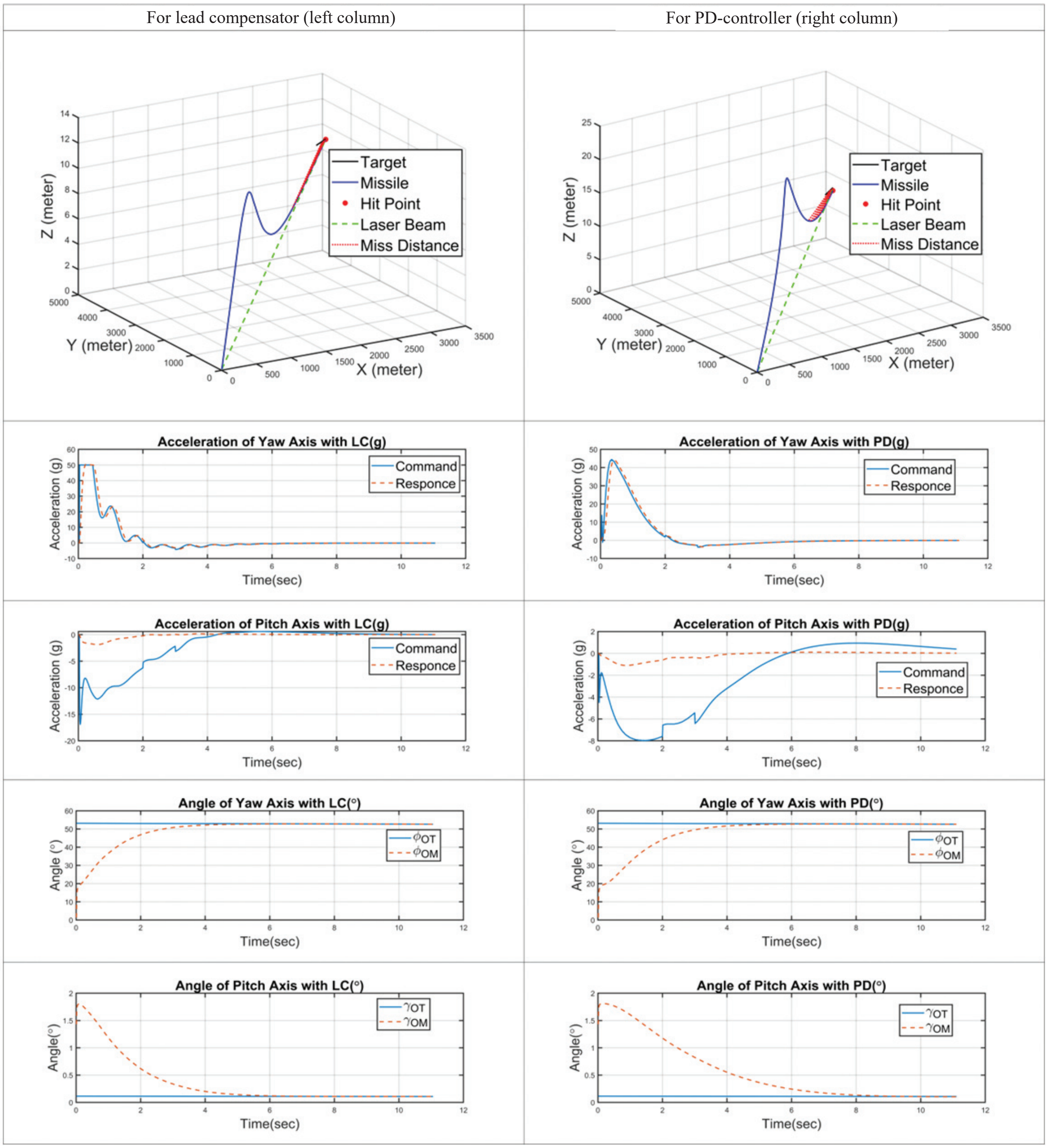

Figure 5. Results for scenario-2 (In order from top to bottom: 3D target and ammunition movements, yaw axis accelerations, pitch axis accelerations, yaw axis LOS angle changes, pitch axis LOS angle changes).

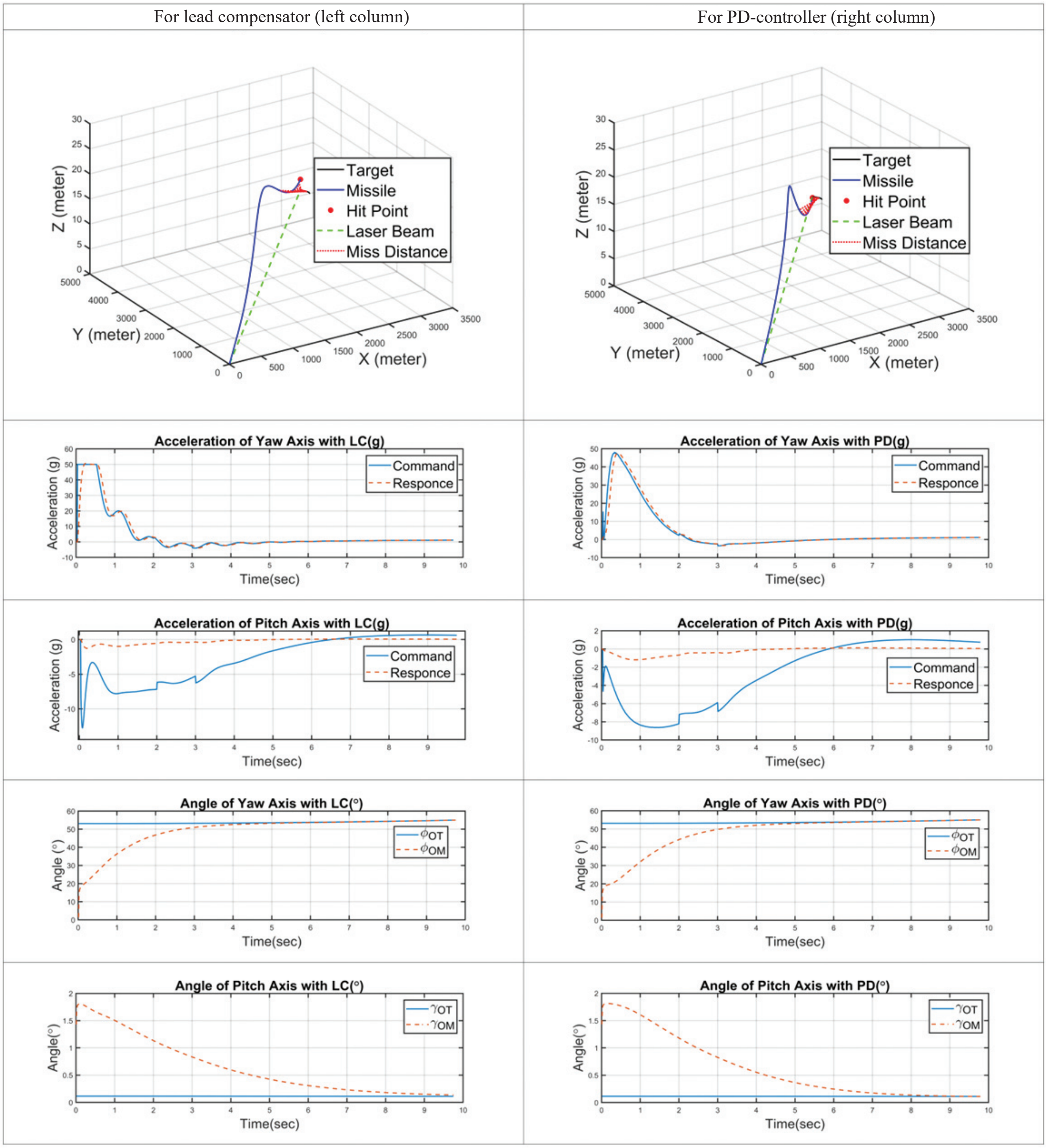

Figure 6. Results for scenario-3 (In order from top to bottom: 3D target and ammunition movements, yaw axis accelerations, pitch axis accelerations, yaw axis LOS angle changes, pitch axis LOS angle changes).

PD-controller. Thus, both controllers can achieve low missing distance against fixed targets and systems moving without acceleration. It is observed that the PD-controller is more effective against accelerated targets. In all scenarios, the PD-controller is more successful in this system as it can achieve lower missing distances without saturating the system.

4. CONCLUSION

In this study, the laser BR-guidance method is applied to conventional tank ammunition with a diameter of 155 mm to provide precision shooting capability to a tank. While there are many documents on guiding missiles, it is seen that there is not any design study for the guidance of tank ammunition in the open literature. For this purpose, the nonlinear system model including mass and inertia of the ammunition, surface area and friction coefficients, the atmospherically and environmental factors is created. In addition, a lead-compensator and a PD-controller are designed to control the nonlinear system model. The PD controller reduces the overshoot and oscillations, generating less compelling accelerations to the control surfaces than the lead compensator, especially in scenarios where the target moves at constant speed and maneuvers with acceleration. Also, it is observed that the PD-controller is more effective against accelerated targets. In order to transfer the results to a real application, the accelerations obtained generally need to be produced by servomotors that will drive the control surfaces. At the end of the study, it is seen that both controllers can produce lateral accelerations within limits without reaching high saturation.

In future studies, first of all, the designed nonlinear model will be detailed with additional effects and will be brought closer to reality. Then, advanced control methods will be offered on the autopilot to reduce the missing distance, maximum and average accelerations, and to control them more stable. For this purpose, detailed stability analyses will also be included in the next study.

REFERENCES

1. Gözde, H. & Ozden, S. Adaptive true proportional navigation guidance based on heuristic optimization algorithms. *Def. Sci. J.,* 2021, **71**(2), 271-281. doi:10.14429/dsj.71.16218
2. Zarchan, P. Tactical and strategic missile guidance (3rd ed.). American Institute of Aeronautics and Astronautics, Virginia, USA, 1997, pp. 193-201
3. Siouris, George M. Missile guidance and control systems. Springer, New York, USA, 2003, pp. 164.
4. Zhou, Q.; Yi, J.; Zhou, X. & Hao, X. Laser beam riding guided system principle and design research. *In* Proceedings of Selected Papers of the Photoelectronic Technology Committee Conferences, China, 2015. doi: 10.1117/12.2229234
5. Maryniak, J.; Edyta L.K.; Krzysztof W. & Krzysztof S. Modeling of spatial motion of an automatically controlled beam-riding guided missile in terms of the Maggi equations. *In* Proceedings of Atmospheric Flight Mechanics Conference and Exhibit, San Francisco, California, 2012. doi: 10.2514/6.2005-6038.
6. Papastavridis, J.G. Maggi's equations of motion and the determination of constraint reactions. *J. Guidance, Control, Dynamics,* 1990, **13**(2), 213-220. doi: 10.2514/3.20539
7. Wang, T. & Zhou, J. Design of integrated guidance-control (IGC) system for beam-riding guided missile. *J. Northwestern Polytech. Uni.versity,* 2009, **27**(2), 173-77.
8. Mingliang, Y.; Zhicheng, H. & Wei C. Laser beam riding artillery missiles guidance device is designed. *In* Proceedings of 7th International Symposium on Advanced Optical Manufacturing and Testing Technologies, Harbin, China, 2014. doi:10.1117/12.2073322
9. Zhou, Q.; Haifeng X.; Xin, S. & Kun, Y. The study of laser beam riding guided system based on 980nm diode laser. *In* Proceedings of Applied Optics and Photonics, China, 2015. doi: 10.1117/12.2201168
10. Wang, P.; Jialin A.; Wenbin Y. & Yudian A. Generation method of laser beam riding guidance information field based on optical phased array. *In* Proceedings of International Conference on Electronic Information Technology and Computer Engineering, online, 2018. doi: 10.1051/matecconf/201823204045
11. Ouda, A.; El-Sheikh, G.; Elhalwagy, Y. & Ashry, M. Robust CLOS Guidance and Control: Part-1: System Modeling and Uncertainty Evaluation. *In* Proceedings of Aerospace Sciences & Aviation Technology Conference, Cairo, Egypt, 2011. doi: 10.21608/asat.2011.23218
12. Szilvassy, L. Aviation anti-tank missile AT-16 (9A4172). *Aeronautical Sci. Bull.*, 2014, **3**, 28-33.
13. Parayil, A. & Ratnoo, A. Cooperative beam-rider guidance for unmanned aerial vehicle rendezvous. *J. Intelligent Rob. Syst.,* 2019, **95**(2), 585-99. doi:10.1007/s10846-018-0873-x
14. Leopard 2 Blueprint - Download Free Blueprint for 3D Modeling, https://drawingdatabase.com/leopard-2/ [Accessed on 08 June 2021]
15. Implement 1976 COESA lower atmosphere - Simulink, https://www.mathworks.com/help/aeroblks/coesaatmospheremodel.html [Accessed on 08 June 2021]
16. Lee, Y-L.; Chen, K-Y. & Liao, S-J. Using proportional navigation and a particle swarm optimization algorithm to design a dual mode guidance. *Comput. Electr. Eng.*, 2016, **54**, 137–146. doi:10.1016/j.compeleceng.2016.01.025
17. Baranowski, L. Effect of the mathematical model and integration step on the accuracy of the results of computation of artillery projectile flight parameters. *Bull. Polish Acad. Sci.: Tech. Sci.,* 2013, **61**(2), 475-84. doi:10.2478/bpasts-2013-0047
18. Balon, R., & Komenda, J. Analysis of the 155 mm ERFB/BB projectile trajectory. *Adv. Military Technol.*, 2006, **1**, 91-114.
19. Defense Technical Information Center. 1958. DTIC AD0209134: A Drag Coefficient, KD, based ONT 155MM shell, HE, M101. http://archive.org/details/DTIC_AD0209134 [Accessed on 08 June 2021]
20. Baranowski, L. Numerical testing of flight stability of spin-stabilized artillery projectiles. *J. Theoretical Appl. Mech.*, 2013, **51**, 375-85.
21. Heng, L.; Gao, G.X.; Walter, T.& Enge, P. Statistical Characterization of GPS Signal-In-Space Errors. *In* Proceedings of the International Technical Meeting of the Institute of Navigation, San Diego, CA, 2011.

CONTRIBUTORS

Mr Mehmet Kum graduated from KTO Karatay University, Department of Mechatronic Engineering in 2016. He is working as a research engineer in The Scientific and Technological Research Council of Turkey (TUBITAK), Defence Industries Research and Development Institute since 2016. His research fields are electronic warfare, infrared systems, guidance and control, seeker design, and mechanical design.
Contribution in the current study, he studied theoretical background, modelling, simulations and obtained the results.

Dr Haluk Gözde completed PhD from Gazi University, Department of Electrical and Electronics Engineering in 2010. He is an Associate Professor in National Defence University, Turkish Military Academy, Department of Electronics and Communication Engineering since 2016. His research fields are artificial intelligence based automatic control applications, dynamics and control of power systems and tactical missile guidance algorithms. He has many articles, book chapters and conference papers to his credit.

Contribution in the current study, he provided his guidance and suggestion to theoretical background, modelling of the guidance system and interpretation of the results.

Dr Semih Özden received his PhD from Gazi University, Department of Electrical and Electronics Engineering in 2013. He is an Assistant Professor in National Defence University, Turkish Military Academy, Department of Electronics and Communication Engineering since 2019. His research interests include artificial intelligence and heuristic algorithms based automatic control applications, embedded systems, power system applications and control techniques of electrical machines. He is the author of over 20 technical publications and conference proceedings.

Contribution in the current study, he studied theoretical background, and interpret the models and results.